

# THE FLOW OF A UNIFORM STREAM OVER A SEMI-INFINITE VERTICAL FLAT PLATE WITH UNIFORM SURFACE HEAT FLUX

GRAHAM WILKS

Department of Mathematics, University of Strathclyde, 26 Richmond Street, Glasgow G1 1XH, Scotland

(Received 26 September 1973 and in revised form 12 November 1973)

**Abstract**—The effect of buoyancy forces on the boundary-layer flow over a semi-infinite vertical flat plate is investigated. The buoyancy forces are favourable, resulting from a uniform flux of heat from the surface of the plate, and their interaction with the boundary-layer flow associated with a uniform stream is examined. Two series solutions are obtained, one valid near the leading edge and the other downstream. An accurate numerical method is used to describe the flow in the region where the series are not valid. Comparison of results leads to some confidence in the merit of the series solutions for Prandtl number of  $O(1)$ .

## NOMENCLATURE

$a$ , velocity of sound;  
 $f$ , non-dimensional stream function near leading edge;  
 $f_i (i = 0, 1, 2)$ , series components of  $f$ ;  
 $\tilde{f}$ , non-dimensional stream function downstream;  
 $\tilde{f}_i (i = 0, 1, 2)$ , series components of  $\tilde{f}$ ;  
 $\bar{F}_n$ , complementary function downstream;  
 $g$ , acceleration due to gravity;  
 $Gr$ , Grashof number,  $\frac{g\beta\Delta Tx^3}{\nu^2}$ ;  
 $\bar{H}_n$ , complementary function downstream;  
 $k$ , thermal conductivity;  
 $Nu$ , Nusselt number,  $\frac{qx}{k\Delta T}$ ;  
 $Q$ , heat-transfer coefficient;  
 $Re$ , Reynolds number,  $\frac{Ux}{\nu}$ ;  
 $T$ , temperature;  
 $T_0$ , temperature of ambient fluid;  
 $T_w$ , local temperature at the plate;  
 $\Delta T$ ,  $T_w - T_0$ ;  
 $u, v$ , velocity components along and normal to the plate;  
 $U$ , uniform stream velocity;  
 $x$ , distance along the plate;  
 $y$ , distance normal to the plate.

## Greek symbols

$\beta$ , coefficient of thermal expansion;  
 $\delta_2$ , momentum thickness;  
 $\delta_T$ , temperature thickness;  
 $\theta$ , non-dimensional temperature near leading edge;  
 $\theta_i (i = 0, 1, 2)$ , series components of  $\theta$ ;  
 $\bar{\theta}$ , non-dimensional temperature downstream;  
 $\bar{\theta}_i (i = 0, 1, 2)$ , series components of  $\bar{\theta}$ ;  
 $\kappa$ , thermometric conductivity;  
 $\mu$ , an undetermined constant;  
 $\nu$ , kinematic viscosity;  
 $\sigma$ , Prandtl number,  $\frac{\nu}{\kappa}$ ;  
 $\tau_w$ , skin friction coefficient;  
 $\xi$ , non-dimensional coordinate along the plate;  
 $\eta$ , non-dimensional coordinate normal to the plate near the leading edge;  
 $\bar{\eta}$ , non-dimensional coordinate normal to the plate downstream;  
 $\psi$ , stream function.

## 1. INTRODUCTION

THIS paper examines an idealisation of a flow situation which often occurs in practice, namely the fluid flow over a surface from which heat is dissipated almost uniformly. The precise model to be examined is described as follows.

A uniform stream flows over a semi-infinite vertical flat plate, which is fixed with its leading edge horizontal. As a result of a uniform surface heat flux at the plate, heat is supplied to the flow by diffusion and convection. This heating gives rise to buoyant body forces which accelerate the fluid in the boundary layer at the plate thus acting as a favourable pressure gradient. Near the leading edge the boundary layer is formed chiefly by the viscous retardation of the free stream whereas far downstream the flow behaviour in the layer is governed by the buoyancy forces.

The problem is formulated in terms of a characteristic non-dimensional coordinate  $\zeta$  which measures the local relative magnitude of viscous and buoyancy forces. Once  $\zeta$  is established two series expansion solutions, valid in different regions are obtained. To obtain each such series solution a transformation is applied to the governing boundary-layer equations. The nature of the transformation is dictated by the anticipation that near the leading edge the buoyancy forces simply provide a modification to a basically forced convection flow whereas downstream the presence of the free stream is considered as a perturbation on the free convection solution. The asymptotic expansion downstream must be approached with caution in the light of a fundamental difficulty outlined by Stewartson [1] and exemplified by Merkin [2] whilst discussing a previous perturbed free convection solution given by Szewczyk [3]. It is not expected that the regions of validity of the series solutions will overlap. These solutions are therefore supplemented by an accurate numerical solution of the problem. The numerical method is an adaptation of a method used by Terrill [4] and Merkin [2] which starts with velocity and temperature profiles at the leading edge and proceeds, step-by-step, to calculate profiles downstream.

Although the methods given in this paper are general ones results are only presented for the case when the Prandtl number  $\sigma = 1$ . This reflects the time and expense required to perform one full numerical solution. Besides providing precise information for this case, an objective of the work must therefore be to provide an opportunity of assessing the merits of the series solutions which can be obtained relatively speedily and economically.

2. THE PROBLEM

The situation under discussion is illustrated in Fig. 1. In a Cartesian coordinate system a semi-infinite plate occupies the region  $y = 0, x \geq 0$  so that  $x$  measures distance along the plate from a fixed horizontal leading edge  $x = 0$  and  $y$  is measured normally outwards from the plate. Incident upon the plate and in the direction of increasing  $x$  is an isothermal uniform stream of

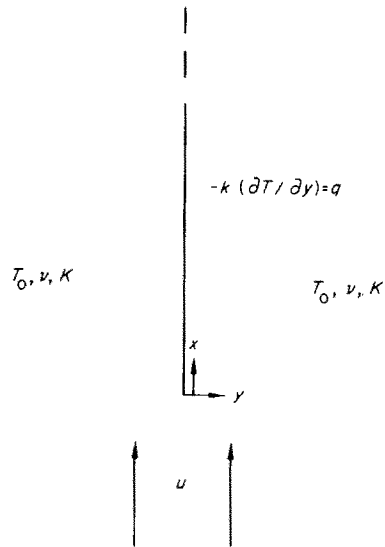


FIG. 1.

velocity  $U$  and temperature  $T_0$ . Favourable buoyancy forces arise as a result of a uniform surface heat flux  $q$  from the plate.

If it is assumed that

$$\frac{U^2}{a^2} \ll \frac{\Delta T}{T_0} \ll 1$$

heating due to viscous dissipation can be neglected and the fluid considered incompressible, so that changes in density are significant only in producing buoyancy forces.  $\nu$  and  $\kappa$  can then be taken as constant and the governing boundary-layer equations expressing conservation of mass, momentum and energy, become

$$\frac{\partial u}{\partial x} + \frac{\partial v}{\partial y} = 0 \tag{1}$$

$$u \frac{\partial u}{\partial x} + v \frac{\partial u}{\partial y} = g\beta(T - T_0) + \nu \frac{\partial^2 u}{\partial y^2} \tag{2}$$

$$u \frac{\partial T}{\partial x} + v \frac{\partial T}{\partial y} = \kappa \frac{\partial^2 T}{\partial y^2} \tag{3}$$

Equations (1)–(3) are to be solved subject to the boundary conditions

$$\begin{aligned} u = v = 0, \quad \frac{\partial T}{\partial y} = -\frac{q}{k} \quad \text{on } y = 0 \\ u \rightarrow U, \quad T \rightarrow T_0 \quad \text{as } y \rightarrow \infty \\ u = U, \quad T = T_0 \quad \text{at } x = 0. \end{aligned} \tag{4}$$

A dimensional analysis of equations (1)–(3) is instrumental in obtaining a non-dimensional characteristic

length scale

$$\xi = \left( \frac{2^3 Gr^2 Nu^2}{5^2 Re^5} \right)^{1/3} = \left( \frac{2^3 g^2 \beta^2 q^2 \nu}{5^2 k^2 U^5} \right)^{1/3} x \quad (5)$$

which reflects the local relative importance of viscous and buoyancy forces. The numerical factors are introduced for convenience. Transformations associated with flow near the leading edge and downstream lead to series expansion solutions in terms of  $\xi^{3/2}$  and  $\xi^{-3/5}$  respectively. The unifying role of the coordinate  $\xi$  is particularly in evidence in the numerical solution when, at  $\xi = 1$ , profiles of velocity and temperature, obtained from an integration of the leading edge form of governing equations, are used as initial profiles for the integration of the asymptotic form of these same equations.

3. NEAR THE LEADING EDGE—SMALL  $\xi$

In this vicinity there is little opportunity for heat from the plate to be taken into the fluid, and the boundary layer is formed mainly by the retardation of the free stream  $U$  by viscosity. This suggests the following transformations

$$\psi = (2\nu Ux)^{1/2} f(\xi, \eta)$$

$$T - T_0 = -\frac{q}{k} \left( \frac{2\nu x}{U} \right)^{1/2} \theta(\xi, \eta)$$

where  $\psi$  is the stream function,

$$\eta = y \left( \frac{U}{2\nu x} \right)^{1/2}$$

and  $\xi$  is as in (5) above.

The boundary-layer equations become

$$\frac{\partial^3 f}{\partial \eta^3} + f \frac{\partial^2 f}{\partial \eta^2} - 5\xi^{3/2} \theta + 2\xi \left\{ \frac{\partial^2 f}{\partial \eta} \frac{\partial f}{\partial \xi} - \frac{\partial f}{\partial \eta} \frac{\partial^2 f}{\partial \xi \partial \eta} \right\} = 0 \quad (6)$$

$$\frac{1}{\sigma} \frac{\partial^2 \theta}{\partial \eta^2} + f \frac{\partial \theta}{\partial \eta} - \theta \frac{\partial f}{\partial \eta} + 2\xi \left\{ \frac{\partial \theta}{\partial \eta} \frac{\partial f}{\partial \xi} - \frac{\partial f}{\partial \eta} \frac{\partial \theta}{\partial \xi} \right\} = 0 \quad (7)$$

with boundary conditions

$$f = \frac{\partial f}{\partial \eta} = 0; \quad \frac{\partial \theta}{\partial \eta} = 1 \quad \text{on} \quad \eta = 0$$

$$\frac{\partial f}{\partial \eta} \rightarrow 1; \quad \theta \rightarrow 0 \quad \text{as} \quad \eta \rightarrow \infty. \quad (8)$$

Solution of equations (6) and (7) are sought by expanding  $f$  and  $\theta$  in series in  $\xi^{3/2}$  in the form

$$f(\xi, \eta) = f_0(\eta) + \xi^{3/2} f_1(\eta) + \xi^3 f_2(\eta) + \dots$$

$$\theta(\xi, \eta) = \theta_0(\eta) + \xi^{3/2} \theta_1(\eta) + \xi^3 \theta_2(\eta) + \dots$$

which, when substituted in equations (6) and (7) and

equating powers of  $\xi^{3/2}$ , yield

$$O(1) \quad f_0''' + f_0 f_0'' = 0$$

$$\frac{1}{\sigma} \theta_0'' + f_0 \theta_0' - \theta_0 f_0' = 0 \quad \left( ' \equiv \frac{d}{d\eta} \right)$$

$$O(\xi^{3/2}) \quad f_1''' + f_1'' f_0 + 4f_1' f_0'' - 3f_0' f_1' - 5\theta_0 = 0$$

$$\frac{1}{\sigma} \theta_1'' + \theta_1' f_0 + 4f_1 \theta_0' - \theta_0 f_1' - 4\theta_1 f_0' = 0 \quad (9)$$

$$O(\xi^3) \quad f_2''' + f_2'' f_0 + 7f_2' f_0'' - 6f_0' f_2' - 5\theta_1 = 0$$

$$= 3f_1'^2 - 4f_1 f_1''$$

$$\frac{1}{\sigma} \theta_2'' + \theta_2' f_0 + 7f_2 \theta_0' - f_2' \theta_0 - 7\theta_2 f_0' = 0$$

$$= 4\theta_1 f_1' - 4\theta_1' f_1$$

with boundary conditions

$$f_0(0) = f_1(0) = f_2(0) = \dots = 0$$

$$f_0'(0) = f_1'(0) = f_2'(0) = \dots = 0$$

$$\theta_0(0) = 1; \quad \theta_1(0) = \theta_2(0) = \dots = 0 \quad (10)$$

$$f_0'(\infty) = 1; \quad f_1'(\infty) = f_2'(\infty) = \dots = 0$$

$$\theta_0(\infty) = \theta_1(\infty) = \theta_2(\infty) = \dots = 0.$$

The forced convection nature of the flow in this region is apparent in the  $O(1)$  system of equations for  $f_0, \theta_0$ . Here  $f_0$  is clearly the Blasius solution for isothermal incompressible viscous flow past a flat plate. The overall system of equations (9) is not amenable to analytic solution and solutions to these two-point boundary value problems must be obtained numerically. Solution is accomplished once values of  $f_i''(0), \theta_i(0) (i = 0, 1, 2, \dots)$  are established which enable boundary conditions at infinity to be satisfied when the equations are integrated outwards from  $\eta = 0$ . Such solutions are readily obtained and are presented in the results.

4. DOWNSTREAM—LARGE  $\xi$

Away from the leading edge buoyancy forces become increasingly important until far downstream the flow will be predominantly one of free convection perturbed by the presence of the free stream. In view of the solution of Sparrow and Gregg [5] for the purely free convection flow under the constant heat flux specification the following transformations are invoked

$$\psi = C_2 x^{4/5} \tilde{f}(\xi, \bar{\eta})$$

$$T - T_0 = -\frac{qx^{1/5}}{kC_1} \bar{\theta}(\xi, \bar{\eta})$$

where

$$\bar{\eta} = \frac{C_1 y}{x^{1/5}}$$

and

$$C_1 = \left( \frac{g\beta q}{2.5 \cdot k\nu^2} \right)^{1/5}$$

$$C_2 = \left( \frac{2^4 5^4 g\beta q \nu^3}{k} \right)^{1/5}.$$

The boundary-layer equations (2) and (3) become

$$\frac{\partial^3 \bar{f}}{\partial \bar{\eta}^3} + 8\bar{f} \frac{\partial^2 \bar{f}}{\partial \bar{\eta}^2} - 6\left(\frac{\partial \bar{f}}{\partial \bar{\eta}}\right)^2 - \bar{\theta} + 10\xi \left\{ \frac{\partial^2 \bar{f}}{\partial \bar{\eta}^2} \frac{\partial \bar{f}}{\partial \xi} - \frac{\partial^2 \bar{f}}{\partial \bar{\eta} \partial \xi} \frac{\partial \bar{f}}{\partial \bar{\eta}} \right\} = 0 \quad (11)$$

$$\frac{1}{\sigma} \frac{\partial^2 \bar{\theta}}{\partial \bar{\eta}^2} + 8\bar{f} \frac{\partial \bar{\theta}}{\partial \bar{\eta}} - 2\bar{\theta} \frac{\partial \bar{f}}{\partial \bar{\eta}} + 10\xi \left\{ \frac{\partial \bar{\theta}}{\partial \bar{\eta}} \frac{\partial \bar{f}}{\partial \xi} - \frac{\partial \bar{f}}{\partial \bar{\eta}} \frac{\partial \bar{\theta}}{\partial \xi} \right\} = 0 \quad (12)$$

with boundary conditions

$$\begin{aligned} \bar{f} = \frac{\partial \bar{f}}{\partial \bar{\eta}} = 0; \quad \frac{\partial \bar{\theta}}{\partial \bar{\eta}} = 1 \quad \text{on} \quad \bar{\eta} = 0 \\ \frac{\partial \bar{f}}{\partial \bar{\eta}} \rightarrow \frac{1}{5} \xi^{-3/5}; \quad \bar{\theta} \rightarrow 0 \quad \text{as} \quad \bar{\eta} \rightarrow \infty. \end{aligned} \quad (13)$$

The perturbation nature of the free stream presence is revealed in the behaviour of  $\partial \bar{f} / \partial \bar{\eta}$  as  $\bar{\eta} \rightarrow \infty$ . To accommodate this boundary condition series solutions of (11) and (12) are sought in the form

$$\begin{aligned} \bar{f}(\xi, \bar{\eta}) &= \bar{f}_0(\bar{\eta}) + \xi^{-3/5} \bar{f}_1(\bar{\eta}) + \xi^{-6/5} \bar{f}_2(\bar{\eta}) + \dots \\ \bar{\theta}(\xi, \bar{\eta}) &= \bar{\theta}_0(\bar{\eta}) + \xi^{-3/5} \bar{\theta}_1(\bar{\eta}) + \xi^{-6/5} \bar{\theta}_2(\bar{\eta}) + \dots \end{aligned}$$

These expansions lead to the following system of equations

$$\begin{aligned} O(1) \quad & \bar{f}_0''' + 8\bar{f}_0 \bar{f}_0'' - 6\bar{f}_0'^2 - \bar{\theta}_0 = 0 \\ & \frac{1}{\sigma} \bar{\theta}_0'' + 8\bar{f}_0 \bar{\theta}_0' - 2\bar{\theta}_0 \bar{f}_0' = 0 \quad \left( ' \equiv \frac{d}{d\bar{\eta}} \right) \\ O(\xi^{-3/5}) \quad & \bar{f}_1''' + 8\bar{f}_0 \bar{f}_1'' + 2\bar{f}_0'' \bar{f}_1 - 2\bar{f}_0' \bar{f}_1' - \bar{\theta}_1 = 0 \\ & \frac{1}{\sigma} \bar{\theta}_1'' + 8\bar{f}_0 \bar{\theta}_1' + 2\bar{f}_1 \bar{\theta}_0' + 4\bar{\theta}_1 \bar{f}_0' - 2\bar{\theta}_0 \bar{f}_1' = 0 \\ O(\xi^{-6/5}) \quad & \bar{f}_2''' + 8\bar{f}_0 \bar{f}_2'' - 4\bar{f}_0'' \bar{f}_2 - \bar{\theta}_2 = -2\bar{f}_1'' \bar{f}_1 \\ & \frac{1}{\sigma} \bar{\theta}_2'' + 8\bar{f}_0 \bar{\theta}_2' - 4\bar{\theta}_0'' \bar{f}_2 - 2\bar{\theta}_0 \bar{f}_2' + 10\bar{\theta}_2 \bar{f}_0' \\ & \quad \quad \quad = -2\bar{f}_1 \bar{\theta}_1' - 4\bar{\theta}_1 \bar{f}_1' \end{aligned} \quad (14)$$

to be solved subject to boundary conditions

$$\begin{aligned} \bar{f}_0(0) = \bar{f}_1(0) = \bar{f}_2(0) = \dots = 0 \\ \bar{f}_0'(0) = \bar{f}_1'(0) = \bar{f}_2'(0) = \dots = 0 \\ \bar{\theta}_0(0) = 1; \quad \bar{\theta}_1(0) = \bar{\theta}_2(0) = \dots = 0 \\ \bar{f}_0(\infty) = 0; \quad \bar{f}_1(\infty) = \frac{1}{5}; \quad \bar{f}_2(\infty) = 0; \quad \dots \\ \bar{\theta}_0(\infty) = \bar{\theta}_1(\infty) \dots = 0. \end{aligned} \quad (15)$$

$O(1)$  solutions of (14) coincide with those of Sparrow and Gregg [5] and describe the flow about a semi-infinite flat plate at whose surface the heat flux is constant.

In establishing the correct form for the series expansion of  $\bar{f}$  and  $\bar{\theta}$  account must be taken of those complementary functions which identically satisfy the boundary conditions at zero and infinity and which are exponentially small when  $\bar{\eta}$  is large. A combination

of them can be added to the solution which will still satisfy all the conditions imposed. It has been shown by Stewartson [1] that the numerical constant multiplying each such complementary function must in some way be associated with the conditions satisfied by the stream function upstream. Moreover, if as often happens, such a complementary function occurs at a stage for which a particular integral is required then the condition of exponential decay cannot be fulfilled unless an additional term, consisting of the complementary function multiplied by a log or log-log term, depending on the case, is added. The numerical factor in this term is to be determined by the condition that the particular integral be exponentially small when  $\bar{\eta}$  is large.

The occurrence of such complementary functions can be investigated as follows. Setting

$$\begin{aligned} \bar{f}(\xi, \bar{\eta}) &= \bar{f}_0(\bar{\eta}) + \xi^{-n} \bar{F}_n(\bar{\eta}) \\ \bar{\theta}(\xi, \bar{\eta}) &= \bar{\theta}_0(\bar{\eta}) + \xi^{-n} \bar{H}_n(\bar{\eta}) \end{aligned}$$

and substituting in equations (11) and (12) reduces the problem to that of ascertaining those values of  $n$  for which the system of equations

$$\begin{aligned} \bar{F}_n''' + 8\bar{f}_0 \bar{F}_n'' + (10n-12)\bar{f}_0' \bar{F}_n' \\ + (8-10n)\bar{f}_0' \bar{F}_n - \bar{H}_n = 0 \quad (16) \\ \frac{1}{\sigma} \bar{H}_n'' + 8\bar{f}_0 \bar{H}_n' + (10n-2)\bar{f}_0' \bar{H}_n \\ + (8-10n)\bar{\theta}_0' \bar{F}_n - 2\bar{\theta}_0 \bar{F}_n' = 0 \quad (17) \end{aligned}$$

has a non-trivial solution subject to the boundary condition

$$\begin{aligned} \bar{F}_n(0) = \bar{F}_n'(0) = 0; \quad \bar{H}_n(0) = 0 \\ \bar{F}_n(\infty) = 0; \quad \bar{H}_n(\infty) = 0 \end{aligned}$$

where the decay of  $\bar{F}_n, \bar{H}_n$  as  $\bar{\eta} \rightarrow \infty$  is to be exponential and  $\bar{f}_0(\bar{\eta}), \bar{\theta}_0(\bar{\eta})$  are the  $O(1)$  solutions of (14).

A full investigation of this problem is beyond the scope of this paper although Stewartson's [6] comments on leading edge shift lead us to suspect a solution for  $n = +1$ . In fact a solution of (16) and (17) which satisfies the boundary conditions proves to be

$$\begin{aligned} \bar{F}_1 = \mu [4\bar{f}_0' - \bar{\eta} \bar{f}_0'] \\ \bar{H}_1 = \mu [\bar{\theta}_0' - \bar{\eta} \bar{\theta}_0'] \end{aligned} \quad (18)$$

where  $\mu$  is as yet an undetermined constant. Since expansion solutions in powers of  $(\xi^{-3/5})$  have been assumed the above eigenvalue solution is not in fact the solution of the homogeneous part of any of the systems of equations in (14). Consequently the introduction of a log term in respect of this complementary function solution is not appropriate. Although the solution has no part to play in ensuring the exponential decay of a particular integral it remains true that arbitrary multiples of it could be added to the full

solution without contravening the boundary conditions other than perhaps upstream. In general such contribution to the asymptotic solution remains arbitrary although associated with some overall property of the flow. Estimates of such contributions can be made by comparing the asymptotic solution with a precise numerical solution and indeed at first sight this would seem to be the opportunity afforded by this investigation. However in this particular case the precise contribution of the complementary function  $\bar{F}, \bar{H}$  can be demonstrated to be identically zero, i.e.  $\mu = 0$ . The integrated form of the energy equation yields

$$\text{i.e.} \quad \int_0^\infty u \frac{\partial T}{\partial x} dy + \int_0^\infty v \frac{\partial T}{\partial y} dy = -\kappa \left( \frac{\partial T}{\partial y} \right)_0 \tag{19}$$

$$\frac{d}{dx} \left[ \int_0^\infty uT dy \right] = \kappa \frac{q}{k}.$$

In terms of  $\bar{f}, \bar{\theta}, \xi$  and  $\bar{\eta}$  this reduces to

$$\text{and thus} \quad \frac{d}{d\xi} \left[ \xi \int_0^\infty \bar{\theta} \frac{\partial \bar{f}}{\partial \bar{\eta}} d\bar{\eta} \right] = -\frac{1}{10\sigma} \tag{20}$$

$$\int_0^\infty \bar{\theta} \frac{\partial \bar{f}}{\partial \bar{\eta}} d\bar{\eta} = -\frac{1}{10\sigma}.$$

If, at this stage, a contribution to the asymptotic solution is assumed and expansions for  $\bar{f}, \bar{\theta}$  read

$$\bar{f}(\xi, \bar{\eta}) = \bar{f}_0(\bar{\eta}) + \xi^{-3/5} \bar{f}_1(\bar{\eta}) + \xi^{-1} \bar{F}_1(\bar{\eta}) + \dots$$

$$\bar{\theta}(\xi, \bar{\eta}) = \bar{\theta}_0(\bar{\eta}) + \xi^{-3/5} \bar{\theta}_1(\bar{\eta}) + \xi^{-1} \bar{H}_1(\bar{\eta}) + \dots$$

the implications of (20) are that

$$O(1) \quad \int_0^\infty \bar{\theta}_0 \bar{f}'_0 d\bar{\eta} = -\frac{1}{10\sigma} \tag{21}$$

$$O(\xi^{-3/5}) \quad \int_0^\infty (\bar{\theta}_1 \bar{f}'_0 + \bar{\theta}_0 \bar{f}'_1) d\bar{\eta} = 0 \tag{22}$$

$$O(\xi^{-1}) \quad \int_0^\infty (\bar{\theta}_0 \bar{F}'_1 + \bar{H}_1 \bar{f}'_0) d\bar{\eta} = 0. \tag{23}$$

Introducing the representation (18) into (23) we have

$$\mu \int_0^\infty \{ [\theta_0(4\bar{f}'_0 - \bar{f}'_0 - \bar{\eta} \bar{f}''_0)] + [\bar{f}'_0(\bar{\theta}_0 - \bar{\eta} \bar{\theta}'_0)] \} d\bar{\eta}$$

$$= 4\mu \int_0^\infty \bar{f}'_0 \bar{\theta}_0 d\bar{\eta} - \mu \int_0^\infty \bar{\eta} \frac{d}{d\bar{\eta}} (\bar{f}'_0 \bar{\theta}_0) d\bar{\eta}$$

$$= 5\mu \int_0^\infty \bar{f}'_0 \bar{\theta}_0 d\bar{\eta} = 0$$

which, in view of (21), implies  $\mu \equiv 0$ .

It is concluded that the solution of the systems of equations (14) are therefore appropriate and numerical solutions of these two-point boundary value problems have been obtained. Details appear in the results.

5. NUMERICAL SOLUTION

A step-by-step method of numerical solution was employed whose accuracy is limited only by the time and space required to perform the calculations on the computer. Derivatives in the  $\xi$ -direction are replaced by differences and all other quantities by averages. The method then establishes, by an iterative scheme, velocity and temperature profiles at a station  $\xi_2$ , downstream of the station  $\xi_1$ , at which profiles are known. For starting the solution, the transformed equations (6) and (7) are appropriate and initial profiles are taken as those similarity solutions of the reduced form of equations (6) and (7), i.e.  $f'_0, \theta_0$ . Since the iteration process fails to converge at  $\xi = 0$  the integration is initiated at  $\xi_1 = 5 \times 10^{-6}$  with an initial step length of  $5 \times 10^{-6}$ . Subsequent step lengths are duly enlarged when the maximum number of iterations needed in going from  $\xi_1$  to  $\xi_2$  is less than four. Downstream the transformed equations (11) and (12) are appropriate. The changeover is most conveniently invoked at  $\xi = 1$ , where  $\eta \equiv \bar{\eta}$ . Thus profiles of temperature and velocity obtained from the integration of the transformed equations (6) and (7) at  $\xi = 1$  are used as initial profiles for the integration, commencing at  $\xi = 1$ , of equations (11) and (12).

Errors arise from using finite differences in both the  $\xi$  and  $\eta$ -directions. The size of truncation errors in the  $\eta$ -direction can be checked using finite difference estimates whilst errors in the  $\xi$ -direction are controlled by prescribing a maximum modulus of deviation between a one-step and a two-step solution between stations  $\xi_1$  and  $\xi_2$ . Profiles obtained from integrating at the half intervals are the ones used as initial profiles for the next full step of the solution. The level of accuracy achieved is governed solely by the limitations on available storage space. In this instance integrations in the  $\eta$ -direction were carried out with

$$\eta, \bar{\eta} = 0.1(0.1)6.4$$

and a maximum modulus of deviation of  $5 \times 10^{-5}$ . An overall accuracy of at least three decimal places is therefore anticipated.

RESULTS ( $\sigma \equiv 1$ )

Series solutions

Numerical solution of equation (9) subject to boundary conditions (10) have been established and appropriate initial values are presented in Table 1.

Table 1

	$f_i''$	$\theta_i$
$i = 0$	0.46960	-1.54064
$i = 1$	5.14956	2.68850
$i = 2$	-19.23852	-20.89185

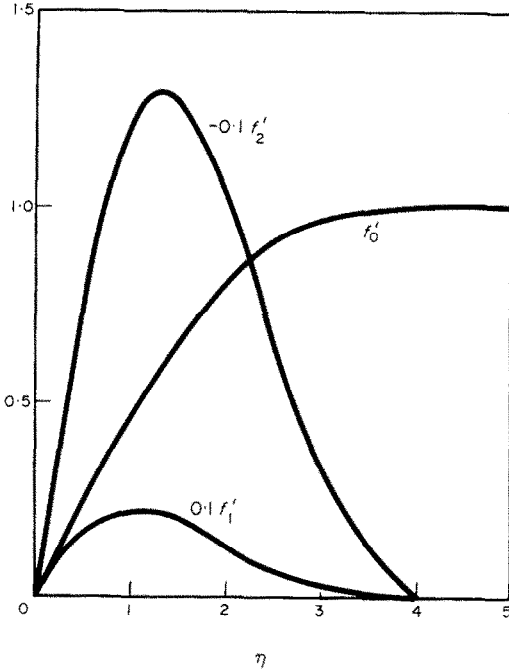


FIG. 2. Velocity functions near the leading edge.

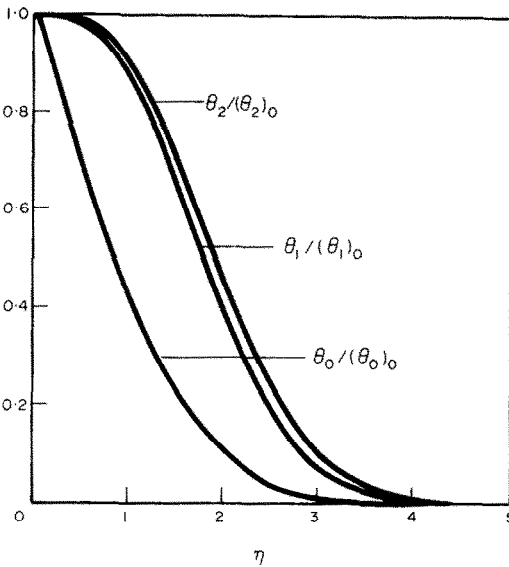


FIG. 3. Temperature functions near the leading edge.

Velocity and temperature profiles associated with the solutions are illustrated in Figs. 2 and 3. We are now able to calculate, in terms of the series expansions, the values of various flow parameters near the leading edge, namely

(i) the skin friction coefficient

$$\tau_w = \left( \frac{5^2 k^2 v^2}{U^4 2^3 g^2 \beta^2 q^2} \right)^{1/6} \left( \frac{\partial u}{\partial y} \right)_{y=0} \quad (24)$$

(ii) the heat-transfer coefficient

$$Q = - \left( \frac{5^2 k^2 v^2 U^2}{2^3 g^2 \beta^2 q^2} \right) \frac{1}{\Delta T} \left( \frac{\partial T}{\partial y} \right)_{y=0} \quad (25)$$

(iii) the momentum thickness

$$\delta_2 = \left( \frac{2^3 g^2 \beta^2 q^2}{5^2 k^2 v^2 U^2} \right)^{1/6} \int_0^\infty \frac{u}{U} \left( 1 - \frac{u}{U} \right) dy \quad (26)$$

(iv) the temperature thickness

$$\delta_T = \left( \frac{2^3 g^2 \beta^2 q^2}{5^2 k^2 v^2 U^2} \right)^{1/6} \int_0^\infty \frac{u}{U} \left( \frac{T - T_0}{\Delta T} \right) dy. \quad (27)$$

In terms of the leading edge variables and solutions associated with Table 1 we have

$$\begin{aligned} \tau_w &= (2\xi)^{-1/2} (f_{\eta\eta})_{\eta=0} \\ &= (2\xi)^{-1/2} (0.46960 + 5.14956\xi^{3/2} \\ &\quad - 19.23852\xi^3 + \dots) \quad (28) \end{aligned}$$

$$\begin{aligned} Q &= - \frac{(2\xi)^{-1/2}}{(\theta)_{\eta=0}} \\ &= (2\xi)^{-1/2} (1.54064 - 2.68850\xi^{3/2} \\ &\quad + 20.89185\xi^3 + \dots)^{-1} \quad (29) \end{aligned}$$

$$\begin{aligned} \delta_2 &= (2\xi)^{1/2} \int_0^\infty \frac{\partial f}{\partial \eta} \left( 1 - \frac{\partial f}{\partial \eta} \right) d\eta \\ &= (2\xi)^{1/2} \{ 0.46960 - 0.58631\xi^{3/2} \\ &\quad + 0.74780\xi^3 + \dots \} \quad (30) \end{aligned}$$

$$\begin{aligned} \delta_T &= (2\xi)^{1/2} \int_0^\infty \frac{\partial f}{\partial \eta} \frac{\theta}{(\theta)_{\eta=0}} d\eta \\ &= (2\xi)^{1/2} \{ 0.32456 + 0.56524\xi^{3/2} \\ &\quad - 0.92747\xi^3 + \dots \} \quad (31) \end{aligned}$$

where Euler-Maclaurin formulae have been used in evaluating integrals appearing in  $\delta_2$  and  $\delta_T$ .

Numerical solutions of equations (14) subject to boundary conditions (15) have also been obtained and appropriate initial values appear in Table 2.

Table 2

	$f_i''$	$\bar{\theta}_i$
$i = 0$	0.54715	-1.18168
$i = 1$	-0.01742	0.13634
$i = 2$	0.02486	0.00995

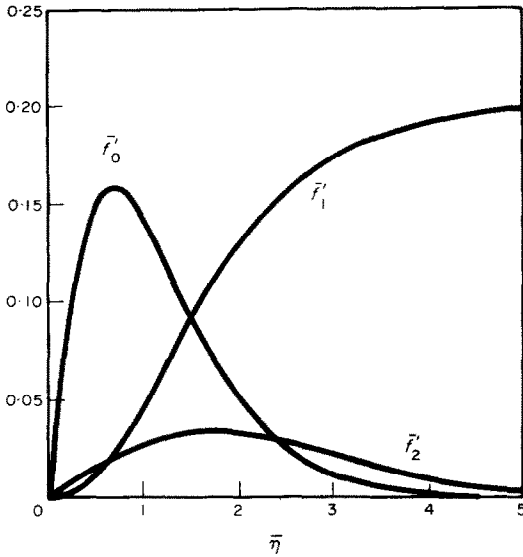


FIG. 4. Velocity functions downstream.

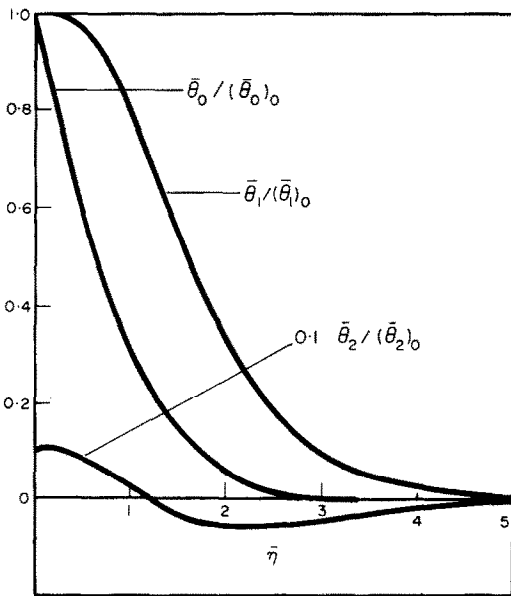


FIG. 5. Temperature functions downstream.

Again velocity and temperature profiles associated with these solutions have been illustrated and appear in Figs. 4 and 5. From the series expansions the values of the flow parameters in terms of the downstream variables and the solutions associated with Table 2 yield

$$\begin{aligned} \tau_w &= 5 \times 2^{-1/2} \xi^{2/5} \left( \frac{\partial^2 f}{\partial \bar{\eta}^2} \right)_{\bar{\eta}=0} \\ &= 5 \times 2^{-1/2} \xi^{2/5} (0.54715 - 0.01742 \xi^{-3/5} \\ &\quad + 0.02486 \xi^{-6/5} + \dots) \end{aligned} \quad (32)$$

$$\begin{aligned} Q &= - \frac{2^{-1/2} \xi^{-1/5}}{(\bar{\theta})_{\bar{\eta}=0}} \\ &= 2^{-1/2} \xi^{-1/5} (1.18168 - 0.13634 \xi^{-3/5} \\ &\quad - 0.00995 \xi^{-6/5} + \dots)^{-1} \end{aligned} \quad (33)$$

$$\begin{aligned} \delta_2 &= 2^{1/2} 5^2 \xi^{7/5} \int_0^\infty \frac{\partial f}{\partial \bar{\eta}} \left( \frac{1}{5 \xi^{3/5}} - \frac{\partial f}{\partial \bar{\eta}} \right) d\bar{\eta} \\ &= 2^{1/2} 5^2 \xi^{7/5} (-0.02751 + 0.02051 \xi^{-3/5} \\ &\quad + 0.01008 \xi^{-6/5} + \dots) \end{aligned} \quad (34)$$

$$\begin{aligned} \delta_T &= 2^{1/2} 5 \xi^{4/5} \int_0^\infty \frac{\partial f}{\partial \bar{\eta}} \frac{\bar{\theta}}{(\bar{\theta})_{\bar{\eta}=0}} d\bar{\eta} \\ &= 2^{1/2} 5 \xi^{4/5} (0.08463 + 0.00977 \xi^{-3/5} \\ &\quad - 0.00177 \xi^{-6/5} + \dots). \end{aligned} \quad (35)$$

Series expansion estimates of the flow parameters have been calculated from (36) to (43) and are included as the dotted line plots in Figs. 6–9.

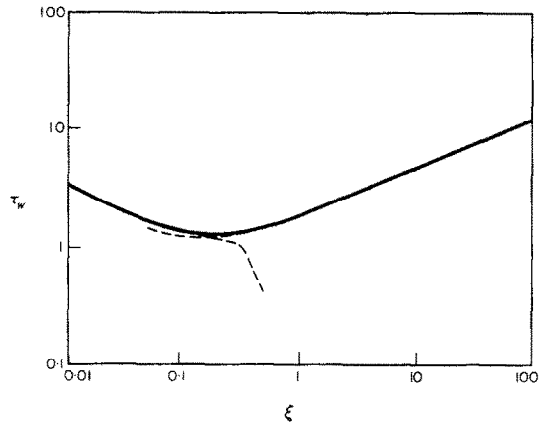


FIG. 6. Skin friction coefficient. — series solutions; — numerical solutions.

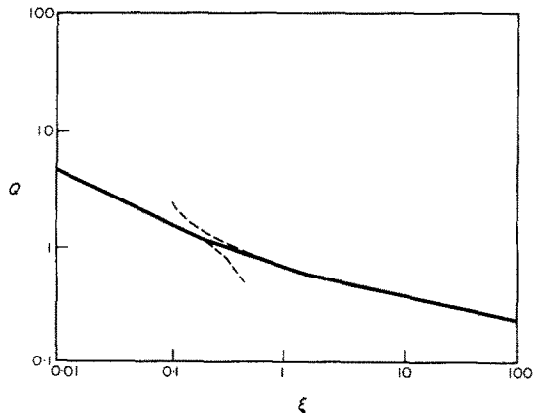


FIG. 7. Heat-transfer coefficient. — series solutions; — numerical solutions.

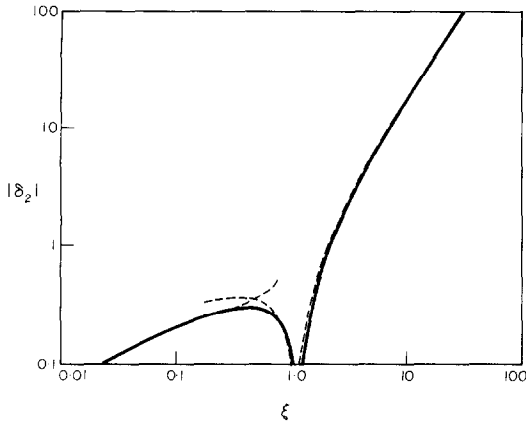


FIG. 8. Momentum thickness. ----- series solutions; ————— numerical solutions.

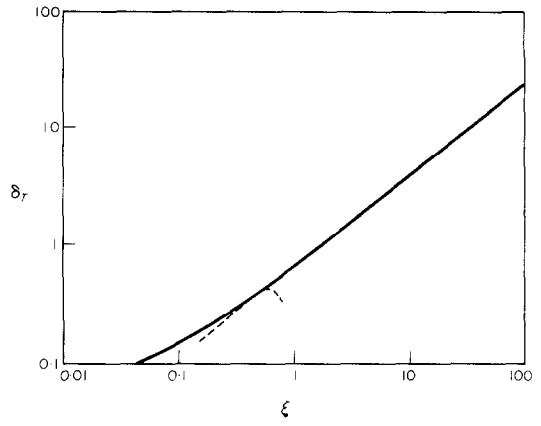


FIG. 9. Temperature thickness. ----- series solutions; ————— numerical solutions.

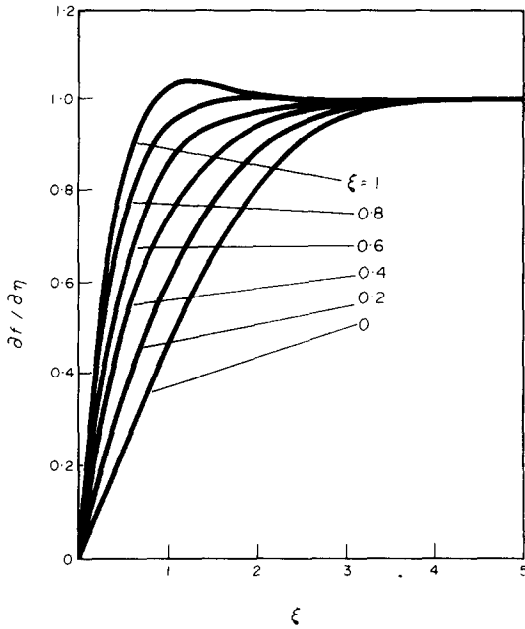


FIG. 10. Velocity profiles from numerical solution.

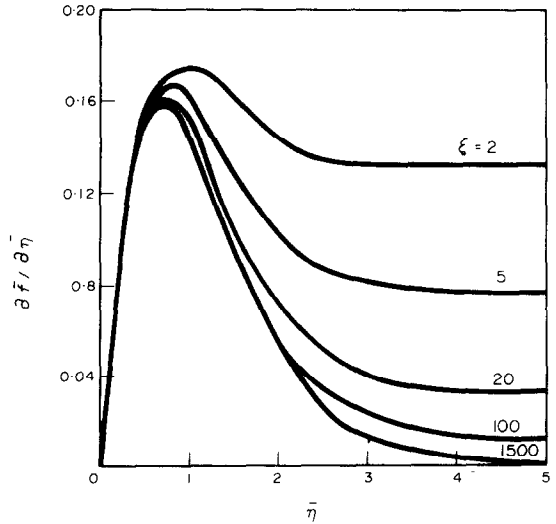


FIG. 11. Velocity profiles from numerical solution.

*Numerical solution*

Results of the full numerical integration of the boundary-layer equations are presented in Tables 3 and 4 in floating point notation. The Tables deal respectively with the two distinct regimes of integration  $0 \leq \xi \leq 1$  and  $1 \leq \xi < \infty$  and list values of the various flow parameters (32)–(38). These results are represented as full line plots in Figs. 6–9. Additional illustrative information is presented in Figs. 10 and 11 where velocity profiles at various stations along the plate are graphed.

**DISCUSSION**

A detailed investigation of the title problem has been outlined and it remains to note the high degree of agreement between the three-term series representations and the exact numerical solutions for Prandtl number unity as illustrated in Figs. 6–9. In all the cases of skin friction, heat transfer, momentum thickness and temperature thickness, estimates overlap over almost the whole range of values of  $\xi$ . Moreover the points at which series representations diverge from the correct solutions are such as to give some confidence that straightforward extrapolations linking these series representations may well be sufficient for practical



Table 3

$\xi$	$\tau_w$	$Q$	$\delta_2$	$\delta_T$
0.00001	1.050 $\alpha$ 2	1.450 $\alpha$ 2	2.100 $\alpha$ -3	1.450 $\alpha$ -3
0.00004	5.251 $\alpha$ 1	7.254 $\alpha$ 1	4.197 $\alpha$ -3	2.901 $\alpha$ -3
0.00016	2.626 $\alpha$ 1	3.627 $\alpha$ 1	8.393 $\alpha$ -3	5.801 $\alpha$ -3
0.00064	1.313 $\alpha$ 1	1.813 $\alpha$ 1	1.678 $\alpha$ -2	1.160 $\alpha$ -2
0.00256	6.573 $\alpha$ 0	9.069 $\alpha$ 0	3.356 $\alpha$ -2	2.321 $\alpha$ -2
0.01024	3.319 $\alpha$ 0	4.541 $\alpha$ 0	6.705 $\alpha$ -2	4.649 $\alpha$ -2
0.02	2.419 $\alpha$ 0	3.260 $\alpha$ 0	9.350 $\alpha$ -2	6.517 $\alpha$ -2
0.03	2.023 $\alpha$ 0	2.672 $\alpha$ 0	1.142 $\alpha$ -1	8.012 $\alpha$ -2
0.04	1.800 $\alpha$ 0	2.324 $\alpha$ 0	1.314 $\alpha$ -1	9.293 $\alpha$ -2
0.05	1.658 $\alpha$ 0	2.089 $\alpha$ 0	1.463 $\alpha$ -1	1.044 $\alpha$ -1
0.06	1.560 $\alpha$ 0	1.917 $\alpha$ 0	1.596 $\alpha$ -1	1.150 $\alpha$ -1
0.07	1.491 $\alpha$ 0	1.784 $\alpha$ 0	1.716 $\alpha$ -1	1.249 $\alpha$ -1
0.08	1.441 $\alpha$ 0	1.678 $\alpha$ 0	1.825 $\alpha$ -1	1.342 $\alpha$ -1
0.09	1.403 $\alpha$ 0	1.591 $\alpha$ 0	1.925 $\alpha$ -1	1.432 $\alpha$ -1
0.10	1.375 $\alpha$ 0	1.519 $\alpha$ 0	2.018 $\alpha$ -1	1.518 $\alpha$ -1
0.12	1.339 $\alpha$ 0	1.402 $\alpha$ 0	2.184 $\alpha$ -1	1.683 $\alpha$ -1
0.14	1.320 $\alpha$ 0	1.314 $\alpha$ 0	2.329 $\alpha$ -1	1.839 $\alpha$ -1
0.16	1.313 $\alpha$ 0	1.243 $\alpha$ 0	2.455 $\alpha$ -1	1.989 $\alpha$ -1
0.18	1.312 $\alpha$ 0	1.185 $\alpha$ 0	2.566 $\alpha$ -1	2.134 $\alpha$ -1
0.20	1.317 $\alpha$ 0	1.137 $\alpha$ 0	2.663 $\alpha$ -1	2.274 $\alpha$ -1
0.24	1.337 $\alpha$ 0	1.060 $\alpha$ 0	2.822 $\alpha$ -1	2.545 $\alpha$ -1
0.28	1.364 $\alpha$ 0	1.002 $\alpha$ 0	2.939 $\alpha$ -1	2.806 $\alpha$ -1
0.32	1.395 $\alpha$ 0	9.551 $\alpha$ -1	3.021 $\alpha$ -1	3.057 $\alpha$ -1
0.36	1.428 $\alpha$ 0	9.169 $\alpha$ -1	3.072 $\alpha$ -1	3.302 $\alpha$ -1
0.40	1.462 $\alpha$ 0	8.847 $\alpha$ -1	3.095 $\alpha$ -1	3.541 $\alpha$ -1
0.48	1.531 $\alpha$ 0	8.335 $\alpha$ -1	3.067 $\alpha$ -1	4.003 $\alpha$ -1
0.56	1.598 $\alpha$ 0	7.939 $\alpha$ -1	2.953 $\alpha$ -1	4.450 $\alpha$ -1
0.64	1.664 $\alpha$ 0	7.621 $\alpha$ -1	2.762 $\alpha$ -1	4.883 $\alpha$ -1
0.72	1.727 $\alpha$ 0	7.358 $\alpha$ -1	2.504 $\alpha$ -1	5.304 $\alpha$ -1
0.80	1.788 $\alpha$ 0	7.135 $\alpha$ -1	2.183 $\alpha$ -1	5.716 $\alpha$ -1
0.88	1.847 $\alpha$ 0	6.946 $\alpha$ -1	1.807 $\alpha$ -1	6.120 $\alpha$ -1
0.96	1.903 $\alpha$ 0	6.776 $\alpha$ -1	1.377 $\alpha$ -1	6.516 $\alpha$ -1
1.00	1.931 $\alpha$ 0	6.699 $\alpha$ -1	1.144 $\alpha$ -1	6.711 $\alpha$ -1

Table 4

$\xi$	$\tau_w$	$Q$	$\delta_2$	$\delta_T$
1.0	1.931 $\alpha$ 0	6.699 $\alpha$ -1	1.144 $\alpha$ -1	6.711 $\alpha$ -1
1.2	2.107 $\alpha$ 0	6.376 $\alpha$ -1	-1.900 $\alpha$ -2	7.667 $\alpha$ -1
1.5	2.291 $\alpha$ 0	6.014 $\alpha$ -1	-2.668 $\alpha$ -1	9.041 $\alpha$ -1
2.0	2.559 $\alpha$ 0	5.593 $\alpha$ -1	-7.859 $\alpha$ -1	1.121 $\alpha$ 0
3.0	3.000 $\alpha$ 0	5.070 $\alpha$ -1	-2.140 $\alpha$ 0	1.525 $\alpha$ 0
4.0	3.364 $\alpha$ 0	4.741 $\alpha$ -1	-3.827 $\alpha$ 0	1.902 $\alpha$ 0
5.0	3.677 $\alpha$ 0	4.506 $\alpha$ -1	-5.786 $\alpha$ 0	2.259 $\alpha$ 0
10.0	4.857 $\alpha$ 0	3.867 $\alpha$ -1	-1.863 $\alpha$ 1	3.878 $\alpha$ 0
15.0	5.717 $\alpha$ 0	3.545 $\alpha$ -1	-3.523 $\alpha$ 1	5.333 $\alpha$ 0
20.0	6.418 $\alpha$ 0	3.336 $\alpha$ -1	-5.470 $\alpha$ 1	6.691 $\alpha$ 0
27.0	7.241 $\alpha$ 0	3.133 $\alpha$ -1	-8.588 $\alpha$ 1	8.483 $\alpha$ 0
36.0	8.128 $\alpha$ 0	2.951 $\alpha$ -1	-1.316 $\alpha$ 2	1.066 $\alpha$ 1
48.0	9.123 $\alpha$ 0	2.780 $\alpha$ -1	-2.007 $\alpha$ 2	1.339 $\alpha$ 1
68.0	1.049 $\alpha$ 1	2.589 $\alpha$ -1	-3.329 $\alpha$ 2	1.766 $\alpha$ 1
100.0	1.225 $\alpha$ 1	2.392 $\alpha$ -1	-5.806 $\alpha$ 2	2.400 $\alpha$ 1
150.0	1.445 $\alpha$ 1	2.203 $\alpha$ -1	-1.038 $\alpha$ 3	3.315 $\alpha$ 1
250.0	1.768 $\alpha$ 1	1.986 $\alpha$ -1	-2.148 $\alpha$ 3	4.982 $\alpha$ 1
450.0	2.238 $\alpha$ 1	1.764 $\alpha$ -1	-4.939 $\alpha$ 3	7.964 $\alpha$ 1
800.0	2.818 $\alpha$ 1	1.571 $\alpha$ -1	-1.113 $\alpha$ 4	1.261 $\alpha$ 2
1500.0	3.624 $\alpha$ 1	1.385 $\alpha$ -1	-2.696 $\alpha$ 4	2.084 $\alpha$ 2
Series	3.604 $\alpha$ 1	1.388 $\alpha$ -1	-2.694 $\alpha$ 4	2.082 $\alpha$ 2

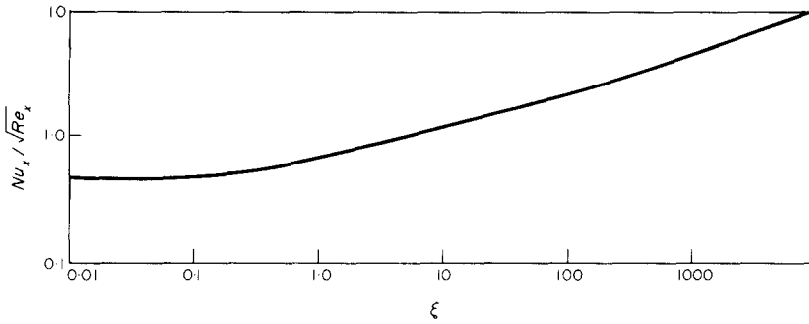


FIG. 12.

purposes. Also noteworthy is the level of agreement between a local similarity analysis and the results of this investigation. In [7] a local similarity analysis was examined and estimates for local Nusselt number

$$\frac{Nu_x}{\sqrt{Re_x}} = -\frac{1}{\theta^*(\xi^*, 0)}$$

presented, where \* refers to the variables of that paper. In Fig. 12 the equivalent exact quantity has been plotted and it is impossible to differentiate graphically the discrepancies between the results of this work and the earlier results over the appropriate range of  $\xi$ . This is an interesting result and further investigations of the correlation between local similarity, series and exact estimates for more extreme values of Prandtl number may be profitable.

## REFERENCES

1. K. Stewartson, On asymptotic expansions in the theory of boundary layers, *J. Math. Phys.* **36**, 173–191 (1957).
2. J. H. Merkin, The effect of buoyancy forces on the boundary-layer flow over a semi-infinite vertical flat plate in a uniform free stream, *J. Fluid Mech.* **35**, 439–450 (1969).
3. A. A. Szewczyk, Combined forced and free-convection laminar flow, *J. Heat Transfer* **C86**, 501–507 (1964).
4. R. M. Terrill, Laminar boundary-layer flow near separation with and without suction, *Phil. Trans. R. Soc.* **A253**, 55–100 (1960).
5. E. M. Sparrow and J. L. Gregg, Laminar free convection from a vertical plate with uniform surface heat flux, *Trans. Am. Soc. Mech. Engrs* **78**, 435 (1956).
6. K. Stewartson, *The Theory of Laminar Boundary Layers in Compressible Fluids*, Oxford Mathematical Monograph. Oxford University Press, Oxford (1964).
7. G. Wilks, Combined forced and free-convection flow on vertical surfaces, *Int. J. Heat Mass Transfer* **16**, 1958–1963 (1973).

ÉCOULEMENT LIBRE UNIFORME SUR UNE PLAQUE PLANE VERTICALE  
SEMI-INFINIE AVEC FLUX THERMIQUE PARIÉTAL UNIFORME

**Résumé**—On étudie l'effet des forces d'Archimède sur l'écoulement de couche limite contre une plaque plane verticale semi-infinie. Ces forces sont favorables dans le cas d'un flux pariétal uniforme de chaleur et on examine leur interaction avec l'écoulement de couche limite. Deux solutions séries sont obtenues, l'une valable près du bord d'attaque et l'autre en aval. Une méthode numérique précise permet de décrire l'écoulement lorsque les séries ne sont pas acceptables. La comparaison des résultats conduit à une certaine confiance en faveur des solutions séries pour un nombre de Prandtl de l'ordre de l'unité.

DIE STETIGE STRÖMUNG ENTLANG EINER HALBUNENDLICHEN, SENKRECHTEN,  
EBENEN PLATTE MIT GLEICHFÖRMIGEM WÄRMESTROM DURCH DIE OBERFLÄCHE

**Zusammenfassung**—Untersucht wird der Einfluß von Auftriebskräften auf die Grenzschichtströmung an einer senkrechten, ebenen Platte. Die von einem gleichmäßigen Wärmestrom aus der Plattenoberfläche verursachten Auftriebskräfte beeinflussen den Wärmeübertragungsvorgang günstig. Ihre Wechselwirkung mit der Grenzschicht einer stetigen Strömung wird behandelt. Es werden zwei Lösungen in Reihendarstellung angegeben. Von diesen gilt eine nahe der Anströmkannte und die andere stromabwärts. Eine genaue numerische Methode wird dort angewandt, wo die Reihenlösungen nicht gelten. Ein Vergleich der Ergebnisse berechtigt zu einigem Vertrauen zu den Reihenlösungen für  $Pr = 1$ .

**ОБ ОДНОРОДНОМ ПОТОКЕ НАД ПОЛУБЕСКОНЕЧНОЙ ВЕРТИКАЛЬНОЙ  
ПЛАСТИНОЙ ПРИ НАЛИЧИИ РАВНОМЕРНОГО ТЕПЛОВОГО ПОТОКА  
НА ПОВЕРХНОСТИ**

**Аннотация** — Исследуется влияние силы Архимеда на течение в пограничном слое вблизи полубесконечной вертикальной пластины. Архимедовы силы, возникающие в результате приложенного к пластине однородного теплового потока, являются значительными; изучается воздействие этих сил на однородной жидкости. Получены решения в виде рядов для передней кромки и для области вниз по потоку. Для описания потока в области, где полученные решения не являются справедливыми, используется точный численный метод. Проведенное сравнение показывает достоверность полученных решений в виде рядов для числа Прандтля  $O(1)$ .